Agricultural and Forest Meteorology 358 (2024) 110220

Contents lists available at ScienceDirect

Agricultural and Forest Meteorology

journal homepage: www.elsevier.com/locate/agrformet

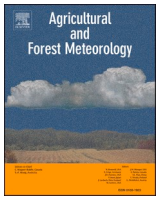

Minor carbon sequestration under nitrogen deposition due to downregulated nitrogen uptake and use efficiency

Song Wang [a,b], Ruiyang Zhang [a], Yuanyuan Huang [a], Yiqi Luo [c], Weinan Chen [c], Yahai Zhang [d], Jinsong Wang [a], Shuli Niu [a,b,*]

[a] Key Laboratory of Ecosystem Network Observation and Modeling, Institute of Geographic Sciences and Natural Research, Chinese Academy of Sciences, Beijing, 100101, China
[b] College of Resources and Environment, University of Chinese Academy of Sciences, Beijing, 100049, China
[c] School of Integrative Plant Science, Cornell University, Ithaca, 14850, NY, USA
[d] State Key Laboratory of Earth Surface Processes and Resource Ecology, Faculty of Geographical Science, Beijing Normal University, Beijing, 100875, China

ARTICLE INFO

Keywords:
Ecosystem adjustment
Nitrogen deposition
Data assimilation
Photosynthetic nitrogen use efficiency
Nitrogen uptake rate

ABSTRACT

Global nitrogen (N) deposition substantially enhances ecosystem carbon cycling but usually results in minor carbon sequestration. The mechanisms underlying the minor stimulation of N deposition on carbon sequestration are not fully understood. Here, we used 22 sets of observations from a gradient N addition experiment with rates at 0, 2, 4, 8, 16, to 32 g $N \cdot m^{-2} \cdot year^{-1}$ in an alpine meadow ecosystem to constrain parameterization of the process-oriented Grassland ECOsystem (GECO) model. Our results indicate that the parameters related to plant N uptake and photosynthetic N use efficiency are proportionally downregulated with the rate of N addition. This is, the higher the rate of N addition, the larger the downward adjustment is in plant N uptake and use efficiency. GECO with parameter values not being adjusted to N treatments simulated higher annual GPP by 16.7 ± 7.1 %, 20.7 ± 6.7 %, 25.2 ± 8.2 %, 23.1 ± 7.0 %, and 49.5 ± 9.1 % under addition rates of 2, 4, 8, 16, and 32 g $N \cdot m^{-2} \cdot year^{-1}$, respectively, in comparison to these with parameter adjustment. Similarly, the ecosystem C storage simulated by GECO model without parameter adjustment was higher by 4.4 ± 2.5 % to 12.0 ± 3.0 % under these with parameter adjustment. Without adjustment of ecosystem physiological processes, such as the plant N uptake rate and use efficiency, Earth system models (ESMs) generally overestimate C uptake and storage under N deposition. Therefore, it is essential to incorporate these adjustments into ESMs to realistically predict global C dynamics under future N enrichment and its feedback to climate change.

1. Introduction

In the last century, global annual nitrogen (N) deposition has increased by ten times and is expected to continue to grow in the future (Lamarque et al., 2005). This growing N deposition can relieve N limitation and stimulate plant growth and potential C sequestration (Du et al., 2014; Fleischer et al., 2019; Lu et al., 2021; Thomas et al., 2010). The direct impact of N-fertilizer is usually reflected as the alleviation of N limitation in earth system models (ESMs) (Gerber et al., 2010; Thomas et al., 2015). Specifically, N addition directly increases the leaf N content, which stimulates photosynthesis by assuming that the maximum rate of carboxylation (Vc_{max}) and the maximum rate of electron transport (J_{max}) are proportional to leaf N content (Koven et al., 2013; Zaehle and Friend, 2010). Therefore, N addition effects simulated by models will continuously improve the productivity and C storage of the ecosystem (Dezi et al., 2010; Thomas et al., 2010; Throop et al., 2004).

However, experimental studies have shown that N addition initially increases plant productivity and biomass until plants' N demand becomes saturated, and growth levels off (Aber et al., 1989; Niu et al., 2016; Song et al., 2017). Other studies have found that N addition typically decreases N use efficiency and plant N uptake rate by influencing their plant functional traits (Jochen, 1988; Meziane and Shipley, 1999), and thus results in ecosystem species adapting to N enrichment (Weese et al., 2015). Those ecosystem adjustments may influence the effects of N addition on C cycling. However, ESMs typically utilize scenario-invariant constants as parameters to represent processes (Luo and Schuur, 2020). Until we have the capability to explicitly represent those changes at the resolved scales, adjustment in parameter values can

* Corresponding author.
E-mail address: sniu@igsnrr.ac.cn (S. Niu).

https://doi.org/10.1016/j.agrformet.2024.110220
Received 17 January 2024; Received in revised form 2 September 2024; Accepted 4 September 2024
Available online 17 September 2024
0168-1923/© 2024 Elsevier B.V. All rights are reserved, including those for text and data mining, AI training, and similar technologies.

typically be used to represent them. However, it is still unclear how N addition may impact biological properties and subsequently affect the prediction of C pools and flux in susceptible vulnerable alpine ecosystems.

Data assimilation, which enables the integration of observations into models, has become increasingly popular in reducing parameter uncertainties and improving model performance (Keenan et al., 2012; Luo et al., 2011; Xu et al., 2006). It can help understand ecosystem C cycles and their response to external disturbances such as N deposition. One advantage of using data assimilation is that it can simulate C cycles within a system with rich data, as demonstrated by studies conducted by Luo et al. (2011) and Shi et al. (2016). Thus, a better comprehension of N enrichment effects on various ecosystem components and their influence on ecosystem C cycles can be achieved. Furthermore, data assimilation can improve model performance by reducing model parameter uncertainties, making the model results more consistent with the observations, and the outputs more reliable (Liang et al., 2018; Xu et al., 2006). Meanwhile, some unresolved scales and changing properties of evolving systems can be represented by model parameterization (Luo and Schuur, 2020). Parameters that are constrained by observation in data assimilation can be utilized to reveal the effects of experimental treatments on the C cycle processes by using parameters that are constrained by different treatments (Liang et al., 2018; Luo and Schuur, 2020; Ma et al., 2023).

In this study, we used data assimilation technique to conduct an inverse analysis of coupled C and N cycles under a gradient N addition experiment (0, 2, 4, 8, 16, 32 g $N{\cdot}m^{-2}{\cdot}year^{-1}$). The primary objectives were to investigate the effects of N enrichment on the C cycle of the alpine meadow ecosystem and to explore the impact of internal mechanism by adjusting plant N uptake and use efficiency. The Bayesian probabilistic inversion was used in this study to estimate C cycle-associated parameters and simulate C pool dynamics for various ecosystem components based on the integral measurements collected at Hongyuan alpine meadow field observation site from 2014 to 2020. The specific questions we addressed in this study are: (1) how did N addition affect plant N uptake rate and photosynthesis N use efficiency? (2) how do the shifts in plant nitrogen uptake and use efficiency influence ecosystem C cycles?

2. Materials and methods

2.1. Site description

The Hongyuan field station is located on the eastern Qinghai-Tibet Plateau (32°84′N, 102°58′E; 3500 m a.s.l), which has a continental plateau frigid temperate monsoon climate. The mean annual precipitation is 747 mm, the mean annual temperature is 1.5 °C, the sunshine duration in a year is about 2000–2400 h, the growing season lasts from April to October. The main vegetation type in the study site is alpine meadow, and the soil type is subalpine meadow soil and boggy soil (Song et al., 2014). This area is dominated by *Deschampsia caespitosa* (Linn.) *Beauv., Koeleria cristata* (Linn.) Pers., *Gentiana sino-ornata* Balf. f., *Potentilla anserina* L., and *Anemone rivularis* Buch.-Ham (Quan et al., 2018).

2.2. Data source

Data sets used to drive the Grassland ECOsystem (GECO) model and used to estimate parameters in this study both were from a N addition experiment and a co-located eddy-covariance measurement system. The eddy covariance system consisted of a three-dimensional sonic anemometer (CSAT3; Campbell Scientific Inc. (CSI), Logan, USA), an open-path CO_2/H_2O infrared gas analyzer (LI-7500A; Li-COR Inc, Lincoln, NE, USA). Data were logged at 10 Hz with a datalogger (CR5000, Campbell Scientific, Utah, USA). Soil volumetric water content (VWC) and soil temperature (Tsoil) were measured simultaneously with the eddy covariance system at a depth of 10 cm every hour using CS655 probe (CSI). Meanwhile, the photosynthetically active radiation was measured with a spherical quantum sensor (LI-190 SB, LI-Cor), wind speed was measured by a cup anemometer (034A-L, RM Young, USA), relative humidity, and air temperature were measured using HMP45C temperature probe (VAISALA, Finland). The fluxes data were processed using the standard methodologies recommended by China FLUX (You et al., 2023; Yu et al., 2008). The N addition experiment near the eddy covariance tower used a random block design with six N addition treatments (N0, N2, N4, N8, N16, N32 represent N addition rates of 0, 2, 4, 8, 16, 32 g $N{\cdot}m^{-2}{\cdot}year^{-1}$, respectively, five replications each). The area of each plot is 8 m × 8 m, and the distance between adjacent quadrats was 3 m. During the growing season from May to September every year, N was added once a month. The method of N addition was spraying, and ammonium nitrate (NH_4NO_3, analytical purity, content ≥ 99 %) was used as N fertilizer. Gross primary productivity (GPP), ecosystem respiration (ER), soil respiration (SR) and heterotrophic respiration (RH) were measured twice a month with static chambers (LI-6400XT, LI-COR Environmental, Lincoln, Nebraska, USA) in plots with different treatments in the growing season from 2014 to 2020. Biometric measurements were made once a year to quantify biomass of plant leaves and roots, standing litter, surface litter, and microbes, soil C content, N content of leaves and roots, standing litter, surface litter, total N content of microbe and soil, and soil inorganic N concentration in all plots.

The data to drive the model included daily soil temperature, soil moisture, photosynthetically active radiation, wind speed, relative humidity, and air temperature from 2014 to 2020. The data assimilated into the GECO model for parameter estimation include C and N contents in leaf, root, standing litter, surface litter, microbial, soil, and autotrophic and heterotrophic respiration at every N addition treatment (supplementary table S1).

2.3. Model

The GECO model was used in this study (Wang et al., 2021, 2022), which has evolved from the Terrestrial ECOsystem (TECO) model (Shi et al., 2016; Xu et al., 2006) with a distinct standing litter pool for grassland ecosystems. There are seven C and N pools and one more mineral N pool in this model. The pools are leaf (X1, N1), roots (X2, N2), standing litter (X3, N3), surface litter (X4, N4), fast (X5, N5), slow (X6, N6), passive soil organic matter (SOM, X7, N7) and mineral N pool. In the GECO model, CO_2 in the atmosphere enters the ecosystem by canopy photosynthesis which is simulated by a two-leaf model (Wang et al., 1998). The plant photosynthetic capacity is limited by the leaf N concentration in the coupled C—N model, reflecting plant investment in photosynthetic machinery for light harvesting and carboxylation rates (Leuning et al., 1995; Walker et al., 2015). Photosynthetic N use efficiency (PNUE) limited by foliage N content as a scalar:

$$SNvcmax = \max\left(\min\left(\exp\left(-\frac{CN_{leaf} - CN_{leaf,0}}{CN_{leaf,0}}\right), 1\right), 0\right) \quad (1)$$

where CN_{leaf} is the estimated C:N ratio of foliage and $CN_{leaf,0}$ is the defined C:N ratio of foliage without N limitation. Some of the photosynthates were used for plants' respiration, and the remaining assimilated C was allocated to leaf (X1) and root (X2) pools. Detritus from the dead plants then flowed into the litter pool, which contained standing litter (X3) and surface litter (X4). Some of the subsurface litter was respired by microbes, while the rest was converted to fast SOM (X5) and slow SOM (X6). The CO_2 released by the decomposition of soil C eventually re-enters the atmosphere. Similarly, plants uptake N from the mineral soil. Subsequently, the uptaken N is distributed to the plant pools and then transferred to the litter and soil pools. The organic N in the seven pools returns to the soil through microbial mineralization. The GECO model uses a matrix-based 1st-order differential equation approach to describe the process of C transfer between ecosystem C

pools as:

$$\frac{d}{dt}\boldsymbol{X}t = \boldsymbol{A}\xi(t)\boldsymbol{K}\boldsymbol{N}_s\boldsymbol{X}(t) + \boldsymbol{b}u(t)$$
$$\boldsymbol{X}(0) = \boldsymbol{X}_0 \quad (2)$$

where $\boldsymbol{X} = (x_1\ x_2\ x_3\ x_4\ x_5\ x_6\ x_7)^T$, in which $x_{(t)}$ represents C pools in leaves, roots, standing litter, surface litter, fast, slow and passive SOM at time *t*. The matrix **A** represents C transfer between pools (Xu et al., 2006). $\boldsymbol{K}$ is a 7 × 7 diagonal matrix with diagonal entries. The elements on the diagonal indicate the C processing rates of each pool ($i = 1, 2, \ldots, 7$). $\boldsymbol{N_s}$ is a 7 × 7 diagonal matrix with diagonal entries, elements on the diagonal indicate the N limiting effects on the pools decomposition rates, which is represented by $\boldsymbol{N_s(i)} = \exp((CN0\text{-}CN(i))/CN0)$ ($i = 1, 2, \ldots, 7$). u represents the C produced by canopy photosynthesis, which is constrained by Eq. (1). $\boldsymbol{b}$ is a vector of partitioning coefficients of photosynthetic products to leaves and roots. $\xi(t)$ is an environmental scalar to account for effects of temperature and humidity on decomposition (Luo et al., 2003).

The N processes can be described by this formula:

$$\frac{d}{dt}\boldsymbol{N}t = \boldsymbol{A}\xi(t)\boldsymbol{K}\boldsymbol{N}_s\boldsymbol{R}^{-1}\boldsymbol{X}(t) + \kappa_\mu N_{min}(t)\boldsymbol{\pi}$$
$$\mathbf{N}(0) = \boldsymbol{N}_0 \quad (3)$$

where $\boldsymbol{N} = (n_1\ n_2\ n_3\ n_4\ n_5\ n_6\ n_7)^T$, in which $n_{(t)}$ represents N pools in leaves, roots, standing litter, surface litter, fast, slow and passive SOM at time *t*. $\boldsymbol{R}$ is a 7 × 7 diagonal matrix with diagonal elements indicating the C:N ratio of each pool. $\boldsymbol{\pi} = (\pi_1\ 1\text{-}\pi_1\ 0\ 0\ 0\ 0\ 0)^T$ is an allocation coefficient vector of N from mineral soil to leaves and roots. κ_μ is N uptake rate of plants, N min(t) is the amount of available N in the soil at time *t*. The dynamic equilibrium of mineral N in soil is determined by the input of mineralization, biological fixation, atmospheric deposition, the output of plant input, leaching, and gaseous N fluxes, which can be described by:

$$\frac{d}{dt}N_{min}t = -(\kappa_u + \kappa_L)N_{min}(t) + \boldsymbol{A}\xi(t)\boldsymbol{\varphi}_1^*\boldsymbol{K}\boldsymbol{N}_s\boldsymbol{R}^{-1}\boldsymbol{X}(t) + F(t)$$
$$N_{min}(0) = N_{min,0} \quad (4)$$

In formula (4), κ_μ and κ_L represent rates of N uptake and N loss, respectively. $\boldsymbol{A}\xi(t)\boldsymbol{\varphi}_1^*\boldsymbol{K}\boldsymbol{N}_s\boldsymbol{R}^{-1}\boldsymbol{X}(t)$ represents N mineralization, $\boldsymbol{\varphi}_1^*$ represents mineralization rate, and $F(t)$ represents N inputs by biological fixation and atmospheric deposition.

In this study, the initial pool sizes of leaves, roots, standing litter, surface litter, fast soil, slow soil, and passive soil pools, were constrained using data in the ambient treatment. The initial pool sizes in the N addition treatment used the same values that were used in the ambient treatment, assuming that no significant difference existed between the ambient and N addition treatment before the treatment started.

2.4. Data assimilation

We used Markov-Chain Monte-Carlo (MCMC) to estimate parameters values of the GECO model. In this method, the targeted parameters are considered as random variables within to a certain prior probability distribution. According to the Bayesian theorem, the prior knowledge about the parameters and the information contained in the data are fused to generate posterior distributions of the parameters (Xu et al., 2006) as

$$P(p|Z) \propto P(Z|p)P(p) \quad (5)$$

In formula 5, $P(p)$ and $P(p|Z)$ represent the prior probability density function (PDF) and posterior probability density function (PPDF) of parameters, respectively. $P(Z|p)$ represents conditional probability density of observation under the prior parameters, which is also called the likelihood function of p. We assume that the random error is normally distributed with zero mean, so the likelihood function can be presented by:

$$P(Z|p) \propto \exp\left\{ -\sum_{i=1}^{17}\sum_{t\in Z_i}\frac{[Z_i(t) - \varphi_i X(t)]^2}{2\sigma_i^2(t)} \right\} \quad (6)$$

In formula 6, Z_i (t) and $\varphi_i X(t)$ represent measured the value and simulated value of observational variable i at time t, and σ_i is the standard deviation of observational variable i. In this study, i from 1 to 17 represents seventeen data sets, which are the C or N contents of leaf, root, standing litter, surface floor, microbe, mineral soil and heterotrophic respiration, soil inorganic N, soil mineralization, plant N uptake and external N input, respectively. φ_i is the mapping vector that maps the simulated state variables.

The Metropolis-Hastings (M-H) algorithm is used as the (Hastings, 1970; Metropolis et al., 1953) MCMC sampler. The initial set of parameters was randomly selected within the priori parameter ranges. At each iteration, a set of parameters (p_{new}) is proposed based on the accepted parameters in the previous iteration (p_{k-1}) we accept the pnew only if $R = \frac{P(p^{new}|Z)}{P(p^{k-1}|Z)} > a$ random number from 0 to 1, or the pnew will be rejected and we let $p_k = p_{k-1}$ to start the sampling of next iteration. The M-H algorithm will be repeated until 300,000 sets of parameter values are accepted, and then all accepted parameter values will be used to construct the probability distribution functions (PDFs) (Weng and Luo, 2011; Xu et al., 2006).

2.5. Model experiments

We chose 100 groups of best-fitted parameters which were picked from approximately 100,000 sets of upgraded parameters to run the GECO model and simulate C dynamics during the period of 2014–2020. In this study, model experiments were conducted to simulate the ecosystem C cycles with and without biological adjustment (Fig. 1). The only difference between the models in this study is the N deposition rate, which was corresponding to the rate of the N addition experiment. The parameters estimated by data assimilation can capture the characteristics of the specific N deposition conditions. Therefore, the biological adjustment effects under N enrichment could also be detected.

In this study, our model was run forward in two scenarios. The first scenario involved an ecosystem with biological responses to N enrichment. In this scenario, we used a model with different N addition rates, with parameters constrained by data from the corresponding N addition treatments. In the second scenario, we examined ecosystem C dynamics without biological adjustment responses to N addition. We used a model with different N addition levels whose parameters were constrained by the data from the ambient N addition treatment. By comparing the two scenarios, we can examine how changes in parameters representing biological processes affect C dynamics at different N-addition levels (Fig. 1).

3. Results

3.1. Model performance on simulating C cycle with and without ecosystem adjustment

The results showed that the simulation of C pools in leaf, standing litter, surface litter, and soil with tuned parameters matched the observations well (supplementary figures S1). And the GPP, ER, SR, RH simulated by the GECO model could fit well with the observations (Fig. 2a, c, e, f, $P < 0.001$). The dynamic of daily GPP simulated in this study could reproduce the seasonal dynamic under different N addition rate, as well (supplementary figure S2).

The simulation of C pools in leaf, standing litter, surface litter, and soil with untuned parameters could not match the observations well (supplementary figure S1). The R^2 and NNSE (Normalized Nash–Sutcliffe Efficiency) values of the simulations with untuned

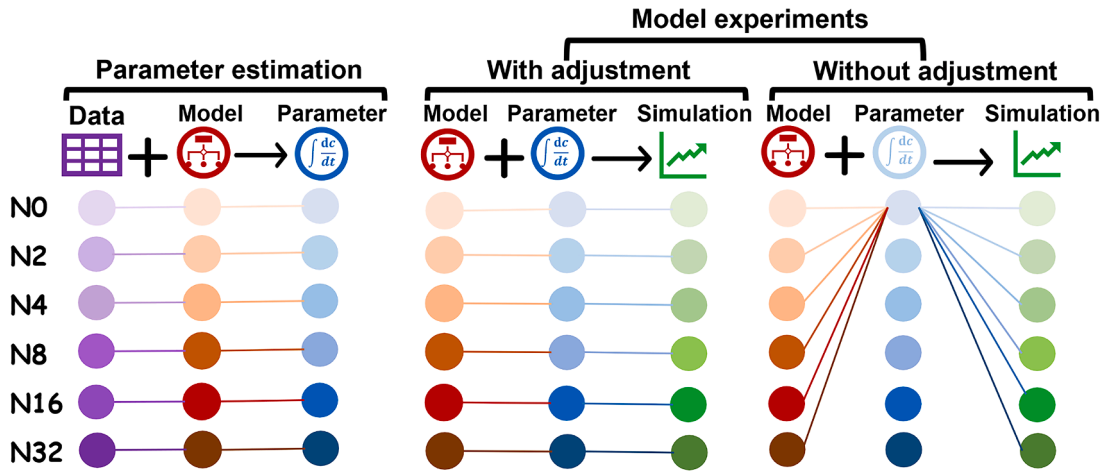

Fig. 1. A concept figure about how to conduct the model experiments in this study. Different shades of purple circles represented different sets data from N0 to N32, which was used to do parameter estimation. Different shades of orange circles represented different models, which had different N deposition rates. Different shades of blue circles represented different sets of parameters estimated by different observations and models. Different shades of green circles represented carbon cycles simulated by different combinations of models and parameters.

parameters were much lower than simulations with tuned parameters, and AIC (Akaike Information Criterion) of the simulations with untuned parameters were higher than simulations with tuned parameters (supplementary table S2). Similarly, the R^2 and NNSE values of GPP, ER, SR, RH simulated with tuned parameters were higher than that simulated with untuned parameters, and AIC values simulated with tuned parameters were lower than that simulated with untuned parameters (Fig. 2 and supplementary table S2).

3.2. Parameters constrained by data-model fusion

Among 18 C-related parameters in this study, eight were well constrained by observations according to their posterior PDFs. These eight well-constrained parameters were C exit rates of root, leaf, standing litter, surface litter, fast SOM, slow SOM, the allocation coefficients of C to root and leaf, leaf photosynthetic efficiency, and plant N uptake rate under all treatments. In these well-constrained parameters, we found that leaf photosynthetic N use efficiency and plant N uptake rate had good relationships with N addition rates (Fig. 3). The correlations between parameter mean values of the posterior distributions and N addition rates including all treatments from 2014 to 2020 were shown in Fig. 3. The leaf photosynthetic efficiency and plant N uptake rate both linearly decreased with the increasing N addition rates ($R^2 = 0.96$, $P < 0.001$; $R^2 = 0.93$, $P < 0.001$).

3.3. Simulated ecosystem carbon pools and fluxes under the gradient nitrogen addition

The comparison of C pools and fluxes from 2014 to 2020 simulated with untuned parameter values vs. with tuned parameters values were shown in Figs. 4 and 5. All simulated C pools using untuned parameter values kept increasing with increasing N addition except the microbe pool, and most simulated C pools using untuned parameter values showed a trend of rise-fall with increasing N addition, which was consistent with the observations (Fig. 4). In most cases, simulated ecosystem C pools using untuned parameter values were higher than those using tuned parameter values.

Similar to C pools, simulated GPP, ER, SR and RH using untuned parameter values enhanced with increasing N addition. Simulated GPP and ER using tuned parameter values showed a trend of rise-fall with increasing N addition, but simulated SR and RH using tuned parameter values showed a trend of decrease with increasing N addition (Fig. 5). Overall, simulated GPP, ER, SR and RH using untuned parameter values were higher than those using tuned parameter values. Compared to the annual GPP simulated by tuned parameters, the GPP value simulated by untuned parameters was higher by 120.0 ± 51.0, 156.2 ± 50.7, 208.7 ± 67.4, 228.9 ± 69.9, 471.4 ± 86.8 g C m^{-2} yr^{-1} (16.7 ± 7.1, 20.7 ± 6.7, 25.2 ± 8.2, 23.1 ± 7.0, 49.5 ± 9.1 %) under N2, N4, N8, N16, N32, respectively. And the simulated leaf, surface litter, microbe, ER, SR, RH also showed similar patterns (Figs. 4 & 5). Compared to the ecosystem C storage simulated by tuned parameters, the ecosystem C storage simulated by un tuned parameters was higher by 179.9 ± 100.2, 23.4 ± 84.0, 84.0 ± 78.5, 383.0.6 ± 84.6, 514.5 ± 129.3 g C m^{-2} (4.4 ± 2.5 %, 0.5 ± 1.9 %, 1.9 ± 1.8 %, 9.0 ± 2.0 %, 12.0 ± 3.0 %) under N2, N4, N8, N16, N32, respectively.

3.4. Ecosystem species change under the gradient nitrogen addition

Plant community varied considerably between N addition treatments (Fig. 6). The relative proportion of *Legumes* had a negative relationship with N addition rates (Fig. 6a). In addition, the biomass of *Legumes* kept decreasing with the increasing N addition (Fig. 6b). Specifically, the proportion and biomass of *Legumes* changed from 3.0 % and 9 g C m^{-2} at N0 treatment to about 0.5 % and 2.5 g C m^{-2} at N32 treatment. And the proportion and biomass of *Legumes* change had good relationship with estimated PNUE and nitrogen uptake rate (Fig. 7). Both PNUE and nitrogen uptake rate increased with higher proportion and biomass of *Legumes*.

4. Discussion

4.1. Ecosystem adjustment to N addition by changing parameters

Plant growth in many regions is limited by soil N availability, particularly in cold regions (Du et al., 2020; Hungate et al., 2003), and N deposition may contribute to a larger C storage in these regions (Chen et al., 2017; Dai et al., 2019; Ren et al., 2010). However, it is well documented that changes in the environment can trigger a variety of biotic responses, spanning short-term physiological adjustments to evolutionary adaptations, such as shifts in the abundance of individual organisms and community composition (Atkins and Travis, 2010; Liang et al., 2018; Ma et al., 2023). N saturation has been observed in various areas and field experiments, where N enrichment caused soil acidification or ion toxicity, resulting in negative impacts on plant growth (Lu et al., 2011; Stevens et al., 2015; Tian and Niu, 2015). Moreover, with the rise in N availability, the ecosystem could potentially experience a

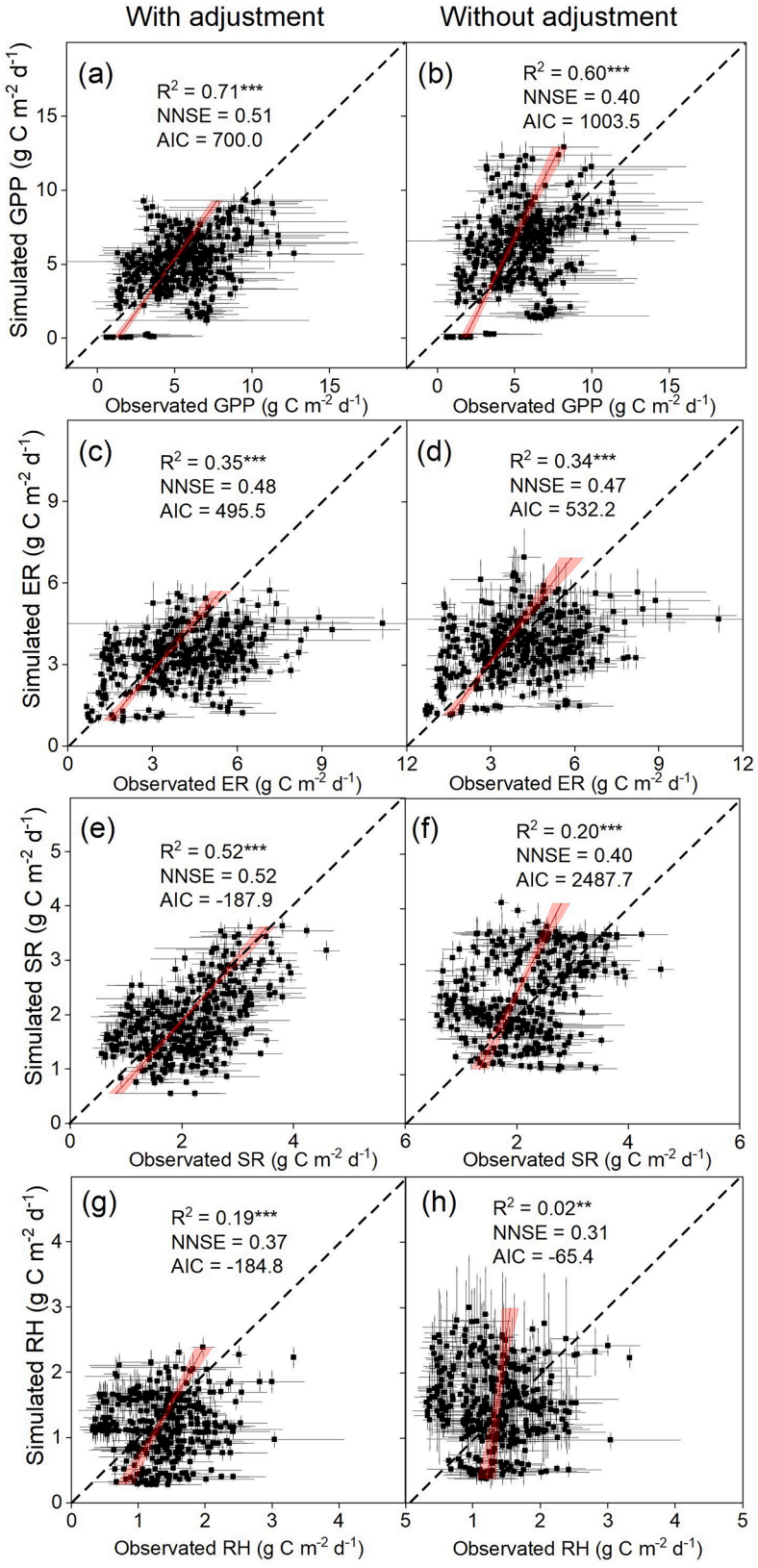

Fig. 2. Comparison of observed and model-simulated (mean ± standard deviation) gross primary productivity (GPP), ecosystem respiration (ER), soil respiration (SR) and heterotrophic respiration (RH) with and without adjusted parameter values.

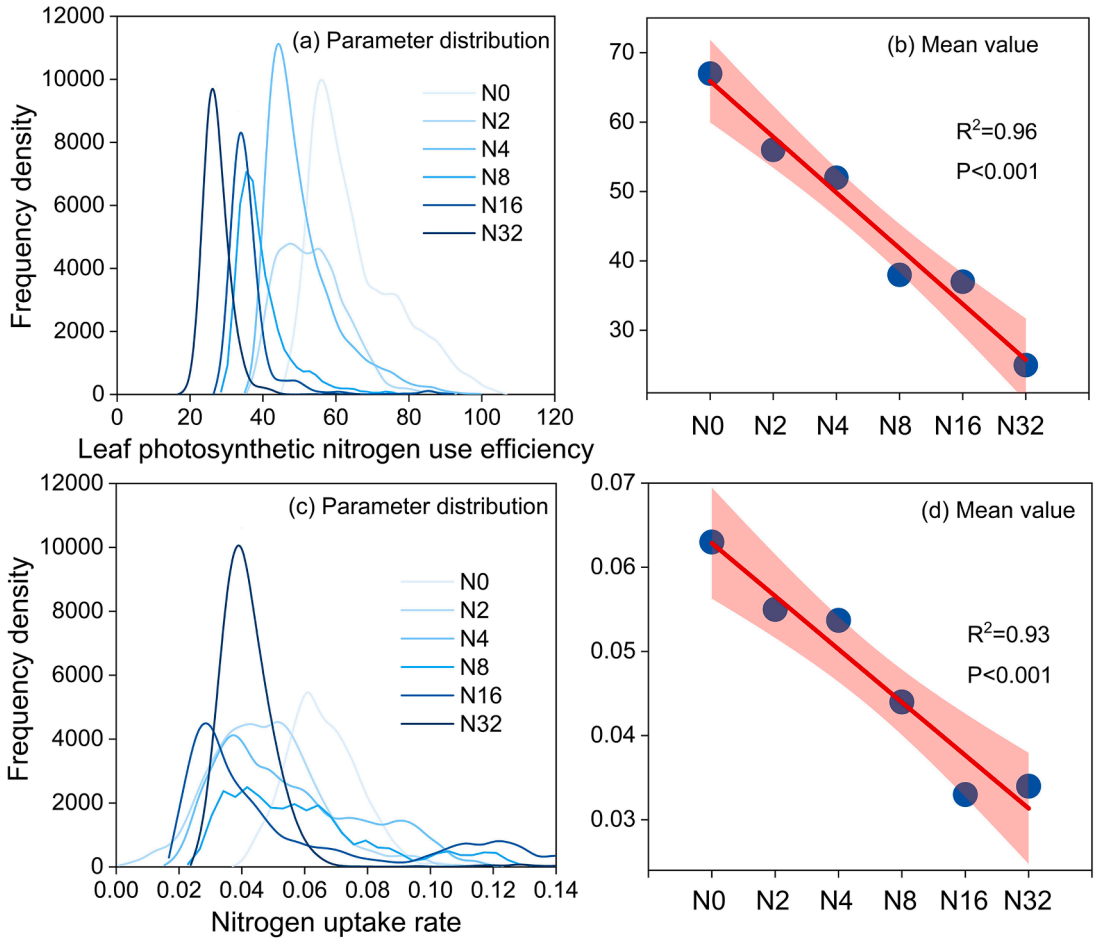

Fig. 3. Posterior distributions of leaf photosynthetic nitrogen efficiency and plant nitrogen uptake rate under different nitrogen addition treatments (a & c). Mean values of leaf photosynthetic efficiency and plant nitrogen uptake rate under different nitrogen addition treatments (b & d).

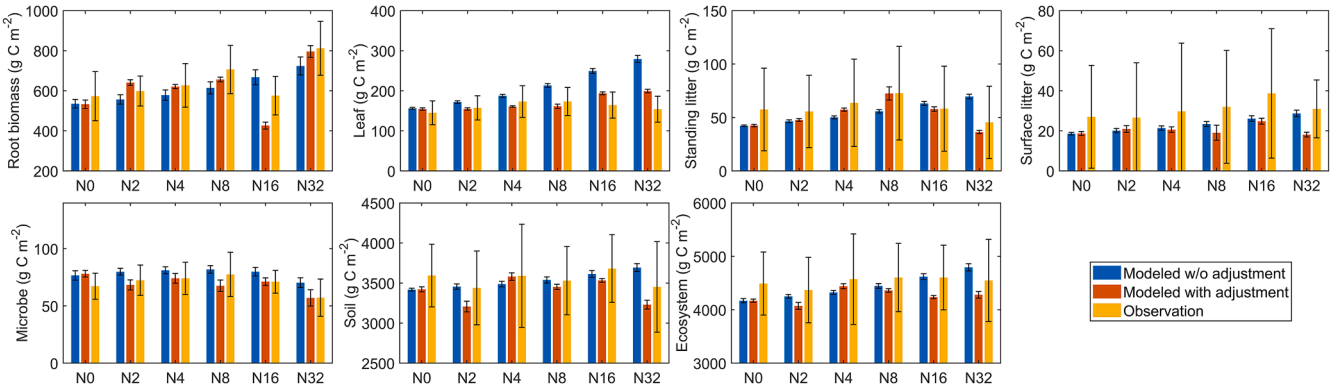

Fig. 4. Simulated and observed annual carbon pools under gradient nitrogen addition treatments. Blue columns are simulated carbon pools without ecosystem nitrogen adjustment and orange columns are simulated carbon pools with ecosystem nitrogen adjustment. Black bars are their standard deviation.

decrease in phosphorus (and other elements) availability, ultimately hindering plant growth and C storage (Bracken et al., 2015; Tessier and Raynal, 2003). We regarded these changes in the ecosystem as adjustment in the ecosystem properties to N enrichment, which are often reflected in changes in model parameter values (Luo and Schuur, 2020).

In this study, we found that the ecosystem adjustment under N enrichment occurred in different levels. At the organ level, we observed a reduction in estimated PNUE with increasing N addition (Fig. 3a). Previous studies have shown that the activation state of Rubisco decreased with increased N content in leaves, and it is suspected that Rubisco acts as a storage protein in leaves with high N content (Cheng and Fuchigami, 2000; Jiang et al., 2015). The decrease in PNUE following N addition in this study can be attributed to the activation state of Rubisco under varying N availability. At the plant level, N addition reduced plant N uptake rate from soil although the total N absorption increased due to the higher soil mineral N content (Fig. 3b). This phenomenon could potentially be explained by that N enrichment alleviating the limitation of N but enhancing the limitation of other elements, which restricted the demand for N in plants (Iversen et al., 2010). At the community or ecosystem level, we observed a substantial

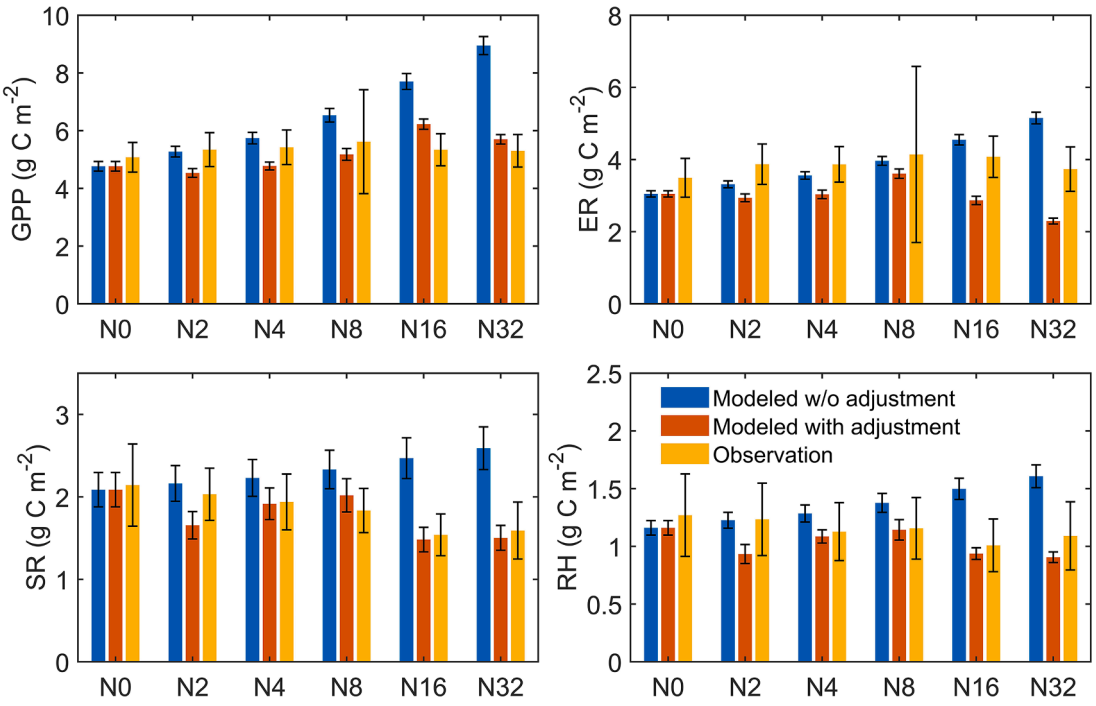

Fig. 5. Simulated and observed annual GPP, ER, SR and RH under gradient nitrogen addition treatments. Blue columns are simulated carbon pools without ecosystem nitrogen adjustment and orange columns are simulated carbon pools with ecosystem nitrogen adjustment. Black bars are their standard deviation.

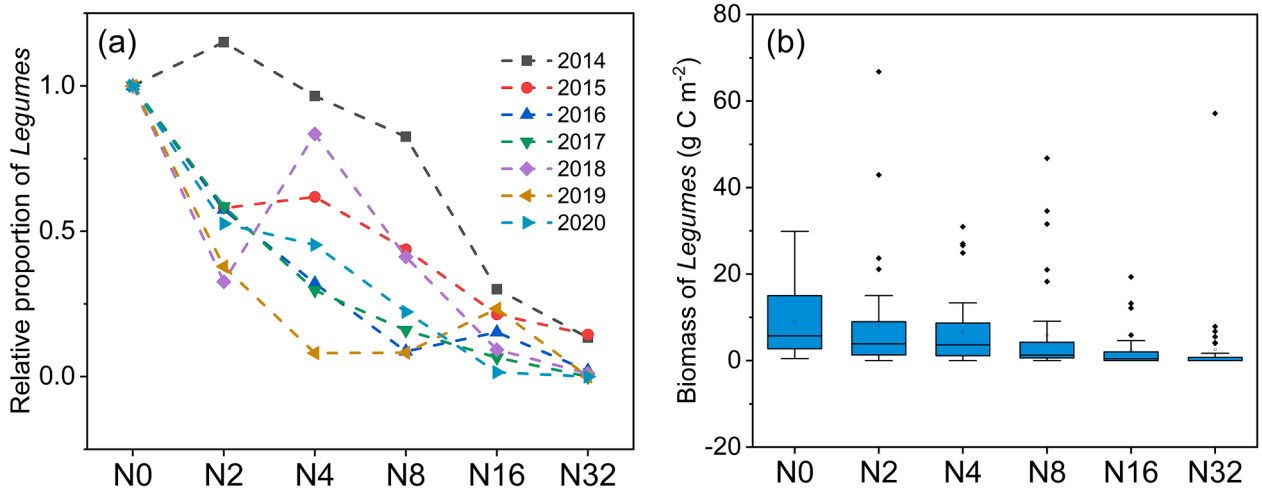

Fig. 6. Nitrogen addition effects on *Legumes*. (a) the relative proportion of *Legumes* under different N addition rates during the study period. (b) the biomass of *Legumes* under different N addition rates.

decrease in biomass and proportion of *Legumes* with the increase of N enrichment. When the soil N content was high, the number, growth, and N fixation activity of *Legumes* root nodules were inhibited (Yamashita et al., 2019). The altered plant community structure will affect the C and N cycle relationship of the community due to variations in the production and N acquisition of species (Pastor and Bridgham, 1999), and this changed plant community structure also reflected as changed parameters in this study. Therefore, the decrease in estimated PNUE and plant N uptake rate induced by N enrichment in our model, explained the ecosystem adjustment to N enrichment. As a consequence, the present study found minor estimation in the C pools and fluxes as N was added, which is consistent with earlier research on the impact of N deposition on C cycles through field experiments (Liu et al., 2021; Niu et al., 2016; Song et al., 2014). These minor estimation in the C pools and fluxes were consequences of ecosystem adjustment under increasing N enrichment.

4.2. Lower simulated carbon sequestration under changing biotic parameters

To evaluate the impact of ecosystem N adjustment on C cycle processes, we conducted model experiments that simulated ecosystem C cycles with and without N adjustment. This was achieved by using adjusted vs. unadjusted parameters under different N addition rates. The results showed that ecosystem N adjustment mitigated the positive effects of N enrichment on ecosystem C fluxes and storage.

Our model experiment results indicated that if we used the fixed parameters under different N addition rates, simulated ecosystem C pools and fluxes kept increasing with increasing N addition, which is consistent with most previous studies using models to simulate the effects of N deposition on C cycles (Dezi et al., 2010; Gu et al., 2015, 2010). Because the photosynthetic rates of these models usually depend

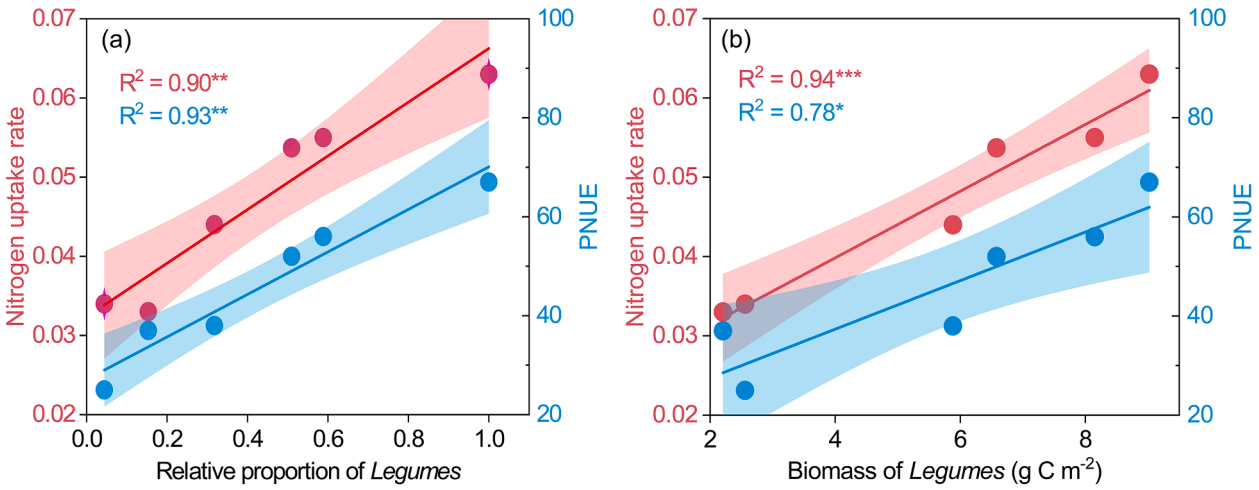

Fig. 7. The relationship between parameters and *Legumes*. (a) the relationship between mean values of leaf photosynthetic nitrogen use efficiency, plant nitrogen uptake rate and the relative proportion of *Legumes*; (b) the relationship between mean values of leaf photosynthetic nitrogen use efficiency, plant nitrogen uptake rate and the biomass of *Legumes*. *when $P < 0.05$, ** when $P < 0.01$, ***when $P < 0.001$.

on leaf N content, which was greatly influenced by N treatment (Gu et al., 2010; Woodward et al., 1995; Zaehle and Friend, 2010). Specifically, in these models, the maximum, light-saturated rate of photosynthesis was determined by leaf N content (Woodward et al., 1995). The maximum carboxylation and electron transport capacities in each canopy layer at 25 °C were also calculated using foliage N content from each layer (Friend and Kiang, 2005; Zaehle and Friend, 2010). In this condition, the C and N cycles were tightly coupled in models through some empirical functions of leaf N content-depended photosynthetic rates. Besides, ESMs usually use fixed parameters to present C and N cycle processes even in different external environments (Friend and Kiang, 2005; Zaehle and Friend, 2010). Hence, the C and N cycles were tightly coupled within the modeling simulation and prediction, resulting in enhanced productivity and biomass with increasing N addition. Nonetheless, this may not reflect the reality of ecosystems.

In general, if adjustment in ecosystem properties was not considered, the model would simulate a much higher GPP in response to N addition, and the simulated leaf, surface litter, microbe, ER, SR, RH also showed similar patterns (Figs. 4 & 5). The overestimated C pools and fluxes simulated by parameters without adjustment than that simulated by parameters with adjustment was mainly due to the decreased PNUE and plant N uptake rate with N addition, which is in line with some previous studies (Jiang et al., 2015; Liang et al., 2020; Wei et al., 2014). Different from the pattern of GPP estimated by different parameters, the simulations of roots, standing litter simulated by parameters with adjustment may be larger than that simulated by parameters without adjustment at some N addition rates. These results indicated that N addition had an intense promotion effect on these C pools at the moderate levels of N addition. And our model may still underestimate the impact of N addition on these C pools at low and moderate levels of N addition treatment.

4.3. Implications for developing ESMs

Ecosystem adjustment under increasing N deposition has important implications for modeling ecosystem C storage and fluxes under global change. A growing number of ESMs incorporate N modules to represent interactions of N cycles with C cycles (Eyring et al., 2016; O'Neill et al., 2016). An important target for involving an N module to ESMs is to represent the C and N coupling relationship and therefore explore its effect on ecosystem productivity and C storage (Zaehle and Dalmonech, 2011). Hence, these studies mainly focused on the effects of N limitation on C uptake and/or C storage, rather than on shifts in C and N coupling relationship (Du et al., 2018; Thornton et al., 2007). The inadequate representation of N cycling processes and also their constraint on C cycling processes led to the overestimation of ecosystem C storage under N deposition, because models cannot realistically simulate the N cycling processes and their impact on C processes (Sutton et al., 2008; Thomas et al., 2013).

Our results indicated that the biological adjustments of ecosystem properties in response to N additions, as reflected by downregulated N uptake and use efficiency decreased the positive effects of N enrichment on ecosystem C storage and productivity. Nevertheless, these biological adjustments to N deposition have not been well represented by ESMs because ecosystem responses to N enrichment may reflect on many complex biotic processes at different scales (i.e., gene, microbe, plant, ecosystem). These biotic processes may involve multiple mechanisms, such as N adjustment of photosynthesis, microbial adaptations, changes in plant functional traits, and shifts in plant communities (Han et al., 2018; Jochen, 1988; Walker et al., 2015; Weese et al., 2015).

Our study highlights the significance of accounting for ecosystem adjustment to N enrichment by using a process-based ecosystem model and in situ data. This novel approach facilitates explorations of how ecosystem C pools and fluxes respond to different N deposition rates. Using N deposition-induced parameter adjustments had a notable impact on simulated ecosystem C pools and fluxes, greatly reducing the productivity and ecosystem C pool storage of the alpine meadow. Thus, ESMs may overestimate C uptake and C storage under N deposition if N deposition adjustments are not implemented in the models. The responses of model parameters to alterations in N deposition rates are consistent with previous research and can be integrated into ESMs. Meanwhile, it is crucial to extend research to encompass additional ecosystem types to validate these algorithms and to gather more data to improve the precision of simulating the response of the global C cycle to N deposition and its feedback to climate change.

5. Conclusion

In this study, by assimilating observational data from an existing experiment at a typical alpine meadow involving a gradient of N addition treatments into a process-oriented GECO model, we investigated how C pools and fluxes responded to long-term gradient N addition treatments, and how ecosystem adjustment affected C pools and fluxes at different N addition rates. We found that ecosystem adjustment to N addition resulted in minor ecosystem productivity and C pool storage under N deposition. And this adjustment was manifested as decreases in the estimated PNUE and plant N uptake rate in our model. Without incorporating the ecosystem adjustment of PNUE and plant N uptake rate, ESMs may overestimate C uptake and C storage under N deposition.

Thus, it is critical to incorporate the ecosystem adjustment of physiological processes into ESMs to realistically predict global C dynamics under future N enrichment and its feedback to climate change.

CRediT authorship contribution statement

Song Wang: Writing – original draft, Software, Methodology. **Ruiyang Zhang:** Writing – review & editing, Data curation. **Yuanyuan Huang:** Writing – review & editing, Methodology. **Yiqi Luo:** Writing – review & editing, Methodology. **Weinan Chen:** Writing – review & editing. **Yahai Zhang:** Writing – review & editing, Software. **Jinsong Wang:** Writing – review & editing. **Shuli Niu:** Writing – review & editing, Resources, Methodology, Conceptualization.

Declaration of competing interest

The authors declare that they have no known competing financial interests or personal relationships that could have appeared to influence the work reported in this paper.

Data availability

Data will be made available on request.

Acknowledgements

This work was financially supported by the National Key Technology R & D Program of China (2022YFF0802102) and the National Natural Science Foundation of China (31988102). We also express our appreciation to Bing Song, Fangyue Zhang, Yingjie Yan, and Jiaming Yang for their help in field and laboratory measurements.

Supplementary materials

Supplementary material associated with this article can be found, in the online version, at doi:10.1016/j.agrformet.2024.110220.

References

Aber, J.D., Nadelhoffer, K.J., Steudler, P., Melillo, J.M., 1989. Nitrogen saturation in Northern forest ecosystems. Bioscience 39 (6), 378–386.
Atkins, K.E., Travis, J.M.J., 2010. Local adaptation and the evolution of species' ranges under climate change. J. Theor. Biol. 266 (3), 449–457.
Bracken, M.E.S., et al., 2015. Signatures of nutrient limitation and co-limitation: responses of autotroph internal nutrient concentrations to nitrogen and phosphorus additions. Oikos 124 (2), 113–121.
Chen, X.P., et al., 2017. The effect of nitrogen deposition rather than warming on carbon flux in alpine meadows depends on precipitation variations. Ecol. Eng. 107, 183–191.
Cheng, L., Fuchigami, L.H., 2000. Rubisco activation state decreases with increasing nitrogen content in apple leaves. J. Exp. Bot. 51 (351), 1687–1694.
Dai, L., et al., 2019. Nitrogen controls the net primary production of an alpine Kobresia meadow in the northern Qinghai-Tibet Plateau. Ecol. Evol. 9 (15), 8865–8875.
Dezi, S., Medlyn, B.E., Tonon, G., Magnani, F., 2010. The effect of nitrogen deposition on forest carbon sequestration: a model-based analysis. Global Change Biol. 16 (5), 1470–1486.
Du, E.Z., et al., 2020. Global patterns of terrestrial nitrogen and phosphorus limitation. Nat. Geosci. 13 (3), 221. -+.
Du, Z.G., et al., 2018. Carbon-nitrogen coupling under three schemes of model representation: a traceability analysis. Geosci. Model. Dev. 11 (11), 4399–4416.
Du, Z., Wang, W., Zeng, W., et al., 2014. Nitrogen deposition enhances carbon sequestration by plantations in northern China. PLoS One 9 (2), e87975.
Eyring, V., et al., 2016. Overview of the coupled model intercomparison project phase 6 (CMIP6) experimental design and organization. Geosci. Model. Dev. 9 (5), 1937–1958.
Fleischer, K., Dolman, A.J., van Der Molen, M.K., et al., 2019. Nitrogen deposition maintains a positive effect on terrestrial carbon sequestration in the 21st century despite growing phosphorus limitation at regional scales. Global Biogeochem. Cycles 33 (6), 810–824.
Friend, A.D., Kiang, N.Y., 2005. Land surface model development for the GISS GCM: effects of improved canopy physiology on simulated climate. J. Climate 18 (15), 2883–2902.
Gerber, S., Hedin, L.O., Oppenheimer, M., Pacala, S.W., Shevliakova, E., 2010. Nitrogen cycling and feedbacks in a global dynamic land model. Global Biogeochem. Cy. 24.
Gu, F.X., et al., 2015. Nitrogen deposition and its effect on carbon storage in Chinese forests during 1981-2010. Atmos. Environ. 123, 171–179.
Gu, F.X., et al., 2010. Modeling the effects of nitrogen deposition on carbon budget in two temperate forests. Ecol. Complex. 7 (2), 139–148.
Han, X., Shen, W., Zhang, J., Muller, C., 2018. Microbial adaptation to long-term N supply prevents large responses in N dynamics and N losses of a subtropical forest. Sci. Total. Environ. 626, 1175–1187.
Hastings, W.K., 1970. Monte-Carlo sampling methods using markov chains and their applications. Biometrika 57 (1), 97. -&.
Hungate, B.A., Dukes, J.S., Shaw, M.R., Luo, Y., Field, C.B., 2003. Atmospheric science. Nitrogen and climate change. Science 302 (5650), 1512–1513.
Iversen, C.M., Bridgham, S.D., Kellogg, L.E., 2010. Scaling plant nitrogen use and uptake efficiencies in response to nutrient addition in peatlands. Ecology 91 (3), 693–707.
Jiang, C., Zu, C., Wang, H.J., 2015. Effect of nitrogen fertilization on growth and photosynthetic nitrogen use efficiency in tobacco (Nicotiana tabacum L.). J. Life Sci. 9 (8), 373–380.
Jochen, A.L., 1988. Relationships between cell surface insulin binding and endocytosis in adipocytes. Am. J. Physiol. 254 (3), E365–E371. Pt 1.
Keenan, T.F., Davidson, E., Moffat, A.M., Munger, W., Richardson, A.D., 2012. Using model-data fusion to interpret past trends, and quantify uncertainties in future projections, of terrestrial ecosystem carbon cycling. Global Change Biol. 18 (8), 2555–2569.
Koven, C.D., et al., 2013. The effect of vertically resolved soil biogeochemistry and alternate soil C and N models on C dynamics of CLM4. Biogeosciences 10 (11), 7109–7131.
Lamarque, J.F., et al., 2005. Assessing future nitrogen deposition and carbon cycle feedback using a multimodel approach: analysis of nitrogen deposition. J. Geophys. Res.-Atmos 110 (D19).
Leuning, R., Kelliher, F.M., Depury, D.G.G., Schulze, E.D., 1995. Leaf nitrogen, photosynthesis, conductance and transpiration - scaling from leaves to canopies. Plant Cell Environ. 18 (10), 1183–1200.
Liang, J., et al., 2018. Biotic responses buffer warming-induced soil organic carbon loss in Arctic tundra. Glob. Chang. Biol. 24 (10), 4946–4959.
Liang, X., et al., 2020. Global response patterns of plant photosynthesis to nitrogen addition: a meta-analysis. Glob. Chang. Biol. 26 (6), 3585–3600.
Liu, G.C., et al., 2021. Long-term nitrogen addition further increased carbon sequestration in a boreal forest. Eur. J. For. Res. 140 (5), 1113–1126.
Lu, M., et al., 2011. Responses of ecosystem nitrogen cycle to nitrogen addition: a meta-analysis. New. Phytol. 189 (4), 1040–1050.
Luo, Y., et al., 2011. Ecological forecasting and data assimilation in a data-rich era. Ecol. Appl. 21 (5), 1429–1442.
Luo, Y., Schuur, E.A.G., 2020. Model parameterization to represent processes at unresolved scales and changing properties of evolving systems. Glob. Chang. Biol. 26 (3), 1109–1117.
Lu, X., Vitousek, P.M., Mao, Q., et al., 2021. Nitrogen deposition accelerates soil carbon sequestration in tropical forests. Proc. Natl. Acad. Sci. 118 (16), e2020790118.
Luo, Y.Q., et al., 2003. Sustainability of terrestrial carbon sequestration: a case study in Duke Forest with inversion approach. Global Biogeochem. Cy. 17 (1).
Ma, S., et al., 2023. Thermal acclimation of plant photosynthesis and autotrophic respiration in a northern peatland. Environ. Res.: Clim. 2 (2), 025003.
Metropolis, N., Rosenbluth, A.W., Rosenbluth, M.N., Teller, A.H., Teller, E., 1953. Equation of state calculations by fast computing machines. J. Chem. Phys. 21 (6), 1087–1092.
Meziane, D., Shipley, B., 1999. Interacting components of interspecific relative growth rate: constancy and change under differing conditions of light and nutrient supply. Funct. Ecol. 13 (5), 611–622.
Niu, S., et al., 2016. Global patterns and substrate-based mechanisms of the terrestrial nitrogen cycle. Ecol. Lett. 19 (6), 697–709.
O'Neill, B.C., et al., 2016. The Scenario Model Intercomparison Project (ScenarioMIP) for CMIP6. Geosci. Model. Dev. 9 (9), 3461–3482.
Pastor, J., Bridgham, S.D., 1999. Nutrient efficiency along nutrient availability gradients. Oecologia 118 (1), 50–58.
Quan, Q., et al., 2018. Transpiration dominates ecosystem water-use efficiency in response to warming in an alpine meadow. J. Geophys. Res.-Biogeo. 123 (2), 453–462.
Ren, Z.W., et al., 2010. Effects of resource additions on species richness and ANPP in an alpine meadow community. J. Plant Ecol. 3 (1), 25–31.
Shi, Z., et al., 2016. Inverse analysis of coupled carbon-nitrogen cycles against multiple datasets at ambient and elevated CO. J. Plant Ecol. 9 (3), 285–295.
Song, B., Niu, S.L., Li, L.H., Zhang, L.X., Yu, G.R., 2014. Soil carbon fractions in grasslands respond differently to various levels of nitrogen enrichments. Plant Soil. 384 (1–2), 401–412.
Song, B., et al., 2017. Initial shifts in nitrogen impact on ecosystem carbon fluxes in an alpine meadow: patterns and causes. Biogeosciences 14 (17), 3947–3956.
Stevens, C.J., et al., 2015. Anthropogenic nitrogen deposition predicts local grassland primary production worldwide. Ecology 96 (6), 1459–1465.
Sutton, M.A., et al., 2008. Uncertainties in the relationship between atmospheric nitrogen deposition and forest carbon sequestration. Global Change Biol. 14 (9), 2057–2063.
Tessier, J.T., Raynal, D.J., 2003. Use of nitrogen to phosphorus ratios in plant tissue as an indicator of nutrient limitation and nitrogen saturation. J. Appl. Ecol. 40 (3), 523–534.
Thomas, R.Q., Brookshire, E.J., Gerber, S.J.G.C.B., 2015. Nitrogen limitation on land: how can it occur in Earth system models? Global Change Biol. 21 (5), 1777–1793.

Thomas, R.Q., Canham, C.D., Weathers, K.C., Goodale, C.L., 2010. Increased tree carbon storage in response to nitrogen deposition in the US. Nat. Geosci. 3 (1), 13–17.
Thomas, R.Q., Zaehle, S., Templer, P.H., Goodale, C.L., 2013. Global patterns of nitrogen limitation: confronting two global biogeochemical models with observations. Glob. Chang. Biol. 19 (10), 2986–2998.
Thornton, P.E., Lamarque, J.F., Rosenbloom, N.A., Mahowald, N.M., 2007. Influence of carbon-nitrogen cycle coupling on land model response to CO2 fertilization and climate variability. Global Biogeochem. Cy. 21 (4) n/a-n/a.
Throop, H.L., Holland, E.A., Parton, W.J., Ojima, D.S., Keough, C.A., 2004. Effects of nitrogen deposition and insect herbivory on patterns of ecosystem-level carbon and nitrogen dynamics: results from the CENTURY model. Global Change Biol. 10 (7), 1092–1105.
Tian, D.S., Niu, S.L., 2015. A global analysis of soil acidification caused by nitrogen addition. Environ. Res. Lett. 10 (2), 024019.
Walker, A.P., et al., 2015. The relationship of leaf photosynthetic traits – Vcmax and Jmax – to leaf nitrogen, leaf phosphorus, and specific leaf area: a meta-analysis and modeling study. Ecology 4 (16), 3218–3235.
Wang, S., Luo, Y.Q., Niu, S.L., 2022. Reparameterization required after model structure changes from carbon only to carbon-nitrogen coupling. J. Adv. Model Earth Sys. 14 (4), 15.
Wang, Y.P., Leuning, R.J.A., Meteorology, F., 1998. A two-leaf model for canopy conductance, photosynthesis and partitioning of available energy. I. Model description and comparison with a multi-layered model. Agric. For. Meteorol. 91 (1–2), 89–111.
Wang, S., Quan, Q., Meng, C., et al., 2021. Experimental warming shifts coupling of carbon and nitrogen cycles in an alpine meadow[J]. J. Plant Ecol. 14 (3), 541–554.
Weese, D.J., Heath, K.D., Dentinger, B.T., Lau, J.A., 2015. Long-term nitrogen addition causes the evolution of less-cooperative mutualists. Evolution (N.Y.) 69 (3), 631–642.
Wei, H.W., Lu, X.T., Lu, F.M., Han, X.G., 2014. Effects of nitrogen addition and fire on plant nitrogen use in a temperate steppe. PLoS One 9 (3), e90057.
Weng, E., Luo, Y., 2011. Relative information contributions of model vs. data to short- and long-term forecasts of forest carbon dynamics. Ecol. Appl. 21 (5), 1490–1505.
Woodward, F.I., Smith, T.M., Emanuel, W.R., 1995. A global land primary productivity and phytogeography model. Global Biogeochem. Cy. 9 (4), 471–490.
Xu, T., White, L., Hui, D.F., Luo, Y.Q., 2006. Probabilistic inversion of a terrestrial ecosystem model: analysis of uncertainty in parameter estimation and model prediction. Global Biogeochem. Cy. 20 (2) n/a-n/a.
Yamashita, N., et al., 2019. Effects of Different Chemical Forms of Nitrogen on the Quick and Reversible Inhibition of Soybean Nodule Growth and Nitrogen Fixation Activity. Front. Plant Sci. 10, 131.
You, C.H., et al., 2023. Inner Mongolia grasslands act as a weak regional carbon sink: a new estimation based on upscaling eddy covariance observations. Agric. For. Meteorol. 342, 11.
Yu, G.-R., et al., 2008. Environmental controls over carbon exchange of three forest ecosystems in eastern China. Global Change Biol. 14 (11), 2555–2571.
Zaehle, S., Dalmonech, D., 2011. Carbon-nitrogen interactions on land at global scales: current understanding in modelling climate biosphere feedbacks. Curr. Opin. Env. Sust. 3 (5), 311–320.
Zaehle, S., Friend, A.D., 2010. Carbon and nitrogen cycle dynamics in the O-CN land surface model: 1. Model description, site-scale evaluation, and sensitivity to parameter estimates. Global Biogeochem. Cy. 24 (1) n/a-n/a.